Relationship between Tropical Heating and Subtropical Westerly Maxima in the Southern Hemisphere during SOP-1, FGGE

JAMES W. HURRELL AND DAYTON G. VINCENT

Department of Earth and Atmospheric Sciences, Purdue University, West Lafayette, Indiana

(Manuscript received 29 September 1989, in final form 4 December 1989)

ABSTRACT

FGGE Level III-b analyses, produced by the Goddard Laboratory for Atmospheres, NASA, are used to investigate the relationship between tropical heating and subtropical westerly maxima in the Southern Hemisphere during SOP-1 (5 January–4 March 1979). The mean state of two 15-day periods is examined, as well as day-to-day variations for the entire 59-day period. In Period 1 (6–20 January), the central South Pacific was extremely active convectively, while in Period 2 (3–17 February), convective activity over the western Indian Ocean was enhanced. Episodes of strong outflow in the tropics, as measured by the upper tropospheric velocity potential, were found to be well correlated with the strengthening and propagation of westerly wind maxima in the subtropics. The average location of the westerly maximum over the South Pacific and Indian oceans was about 16° latitude south, and slightly east, of its corresponding heat source. For a cyclone case study which is presented, however, this distance was considerably less. The response time between the upper level tropical outflow and subtropical westerly enhancement appears to be less than 12 hours; however, an exact temporal scale was difficult to identify.

1. Introduction

The relationship between tropical heating and higher latitude circulations is a topic of great importance and has been investigated on many different space and time scales by numerous authors using both observational and modeling data. A subset of this general topic is the relationship between low latitude heating and westerly wind maxima at similar longitudes but higher latitudes and, specifically, the ability of local Hadley-type circulations induced by the heating to accelerate upper-level westerly flows through the conversion of earth angular momentum (Palmen and Newton 1969; Krishnamurti et al. 1973; Krishnamurti 1979; Chang and Lau 1980, 1982; Physick 1981; Lau et al. 1983; Paegle et al. 1983; Chang and Lum 1985; Nogues-Paegle and Mo 1987, 1988; Nogues-Paegle and Zhen 1987; Chen et al. 1988). Although this link between tropical motions and westerly maxima has been studied on temporal scales as long as monthly and seasonal averages, the focus of the present paper and, consequently, the ensuing literature review, will be on the shorter term relationship in which the higher latitude response to tropical heating is on the order of days to a week.

Over the past decade, numerous observational studies examined short-term interactions between the tropics and midlatitudes centered around the onset of low-level monsoonal cold surges over the South China Sea during northern winter. For instance, Chang and Lau (1980, 1982) were able to relate the strength of the subtropical jet stream over Japan to the 200 mb divergence over the maritime continent of Borneo and Indonesia during peak surge periods. Lau et al. (1983) were able to further substantiate this finding using twice-daily wind analyses from the Winter-MONEX period of December 1978–February 1979. They found that 24 to 36 hours after the onset of cold surges, convection over South Borneo was enhanced and increased divergent meridional flow over East Asia was related to the enhanced convection and the locally intensified Hadley-type overturning centered at 120°E. Moreover, they illustrated that the southerly flow in the upper branch of the East Asia Hadley circulation was responsible for the zonal wind acceleration at the entrance region of the jet over Japan during the surge onset, while eddy momentum flux convergence largely maintained the zonal wind acceleration downstream of the entrance region. Chang and Lum (1985) noted that because cold surges occur as a consequence of increased midlatitude baroclinicity, the observed strengthening of midlatitude westerly wind maxima could be independent of the increased tropical convection and result solely from the enhanced baroclinic development. They used objectively analyzed 200 mb wind data from the Fleet Numerical Oceanographic Center's global band analyses to address this cause and effect problem in short-term tropical–extratropical in-

Corresponding author address: Dr. James Hurrell, Department of Earth and Atmospheric Sciences, Purdue University, West Lafayette, IN 47907.

teractions over eastern Asia and the western Pacific Ocean during the 1983/84 northern winter season. They found a significant positive correlation between midlatitude westerly wind maxima and regions of upper tropospheric tropical divergence at the same longitudes throughout the season. Although the lack of a discernible time lag in the correlations precluded any definite conclusions about the cause and effect problem, their detailed examination of six December 1983 major intensifications of the east Asian westerly jet between 25°N and 40°N provided additional insight. In three of the episodes, deep convection in tropical cyclones located between 0° and 18°N was correlated to an enhancement of the jet on a day-to-day basis. Although the synoptic cause of one episode of enhanced 200 mb tropical divergence was not identified, the remaining two cases were the result of cold surges. From this evidence, Chang and Lum concluded, based on the three tropical cyclone events, that the short-term intensifications of the midlatitude jet were more likely the result, and not the cause, of the tropical–extratropical interaction. Furthermore, they agreed with the previous studies that the poleward moving air in the upper branch of the local Hadley-type circulation, acted upon by the coriolis force, accelerates eastward into the entrance region of the jet. Once formed, the individual westerly wind maxima propagate downstream due to self advection.

Further evidence of a link between tropical divergent circulations and higher latitude westerly wind maxima has been provided by the numerous papers in recent years devoted to the study of low-frequency tropical oscillations with 30–50 day periods, first noted by Madden and Julian (1971, 1972). Unlike studies such as Lorenc (1984) and Krishnamurti et al. (1985), which detected a planetary-scale divergence wave that traverses eastward around the globe with zonal wavenumber 1 and a period of 30–50 days, numerous investigators have examined the propagation of Outgoing Longwave Radiation (OLR) anomalies and have found that strong convection anomalies are confined to the equatorial regions of the Indian Ocean and the western Pacific sector. For example, the results of Murakami and Nakazawa (1985) and Murakami et al. (1986) showed a systematic eastward propagation of low-frequency OLR anomalies most clearly defined between 60°E and the International Date Line (IDL). Weickmann et al. (1985), using ten years of northern winter OLR data, found that the strongest fluctuations at 28–72 day periods traversed eastward between the equator and 15°S from 60°E to 160°E, then shifted rapidly to about 160°W in the vicinity of the South Pacific Convergence Zone (SPCZ). They also found that convection in the SPCZ was out of phase with that in the Indian Ocean. Moreover, they presented observational evidence that this tropical oscillation affected extratropical circulations. Specifically, they found a strengthened Northern Hemisphere upper level subtropical jet over the central Pacific when the tropical oscillation was near the date line and a weakened central Pacific jet when the strong convection was located farther west over Indonesia. In a study of intraseasonal oscillations during Northern Hemisphere summers from 1974–1983, Knutson et al. (1986) also concluded that tropical OLR fluctuations in the 28–72 day spectral band had the greatest amplitude in the Indian monsoon region and the tropical western Pacific, with these two regions having an out-of-phase relationship. In extratropical latitudes, they found the 250 mb zonal wind anomalies along 30°S to be strongly coherent with the tropical OLR anomalies. Nogues-Paegle and Mo (1987) examined the seasonal transition from spring to summer in the Northern Hemisphere using 12 consecutive weekly averages of Global Weather Experiment (FGGE) data starting from 5 May 1979. Their results supported the finding of Knutson et al. (1986). Specifically, they were able to capture two cycles of a propagating easterly divergent wave and fluctuations in OLR consistent with the description of the 30–50 day oscillation. They compared OLR and velocity potential at 5°N with the 200 mb zonal wind at 34°S and found that divergence pulses were followed within one week by accelerations of the westerly wind. These accelerations peaked when the divergence pulse was near 160°E, with maximum subtropical westerly winds at similar longitudes. Their averaging technique, however, precluded any quantification of a temporal response of the subtropical jets to the enhanced tropical latent heat release.

In addition to the aforementioned observational studies, the impact of tropical large-scale organized convection on the wind fields at higher latitudes has been investigated using a wide array of numerical models (e.g., Blackmon et al. 1977; Opsteegh and Van den Dool 1980; Gill 1980; Hoskins and Karoly 1981; Simmons 1982; Lim and Chang 1983; Lau and Lim 1984; Sardeshmukh and Hoskins 1988; Chelliah et al. 1988). One such study of interest to the present investigation is that by Nogues-Paegle and Mo (1988). They used the Goddard Laboratory for Atmospheres (GLA) fourth-order general circulation model (GCM) with real data and examined the transient response of the Southern Hemisphere subtropical jet to tropical forcing during the 1979 Southern Hemisphere winter season. Their study was at least partially motivated by the earlier observational work of Nogues-Paegle and Zhen (1987) which linked episodes of enhanced latent heat release in the Northern Hemisphere tropics for selected cases during June, July and August 1979 to accelerations of Southern Hemisphere subtropical wind maxima at similar longitudes. For the period 25 July through 12 August 1979, Nogues-Paegle and Mo noted that observed accelerations of the 200 mb zonal wind over Australia between 25°S and 35°S were well correlated to enhanced area-averaged rainfall rates in the Northern Hemisphere tropics at similar longitudes.

Specifically, the enhancement episode culminated on 8 August with a zonal wind over Australia of 93 m s^{-1}. Consequently, they performed a 15-day integration initializing the GLA GCM on 1 August 1979 and, in a "full physics" control run, were able to reproduce a peak 200 mb zonal wind of 82 m s^{-1} during 8 August centered over Australia at about 26°S. Moreover, this zonal wind maximum corresponded favorably with increased upper level divergent flow near 6°N, about 50° longitude upstream of the jet during 4 August. Since the control run was successful at simulating the temporal and spatial evolution of the Australian wind maximum, Nogues-Paegle and Mo performed a numerical simulation with suppressed heating over the tropical Pacific from 90°E to 120°W and found that the impact of latent heat release was remotely felt at subtropical latitudes in 2 to 4 days. Although this and many other model studies suggest that a relationship between tropical heating and subtropical jet maxima exists, the question that is often difficult to answer by using the modeling approach is, "What is the initial relationship and/or immediate response (both temporally and spatially) of the circulation pattern to a locally-enhanced heat source?" One must frequently resort to the use of observational studies to answer this question because most large-scale models require a certain amount of time (several hours to a few days) to reach a stable state, especially when diabatic heating represents the main forcing for the evolving circulation.

The purpose of the present paper is to use observational data, provided by FGGE, to diagnose the possible relationships between the heating associated with two convectively active areas of the tropical Southern Hemisphere and the immediate enhancement of a nearby subtropical westerly wind maximum in each region. The regions being examined are the western Indian and the central Pacific oceans, two areas that were convectively out of phase during the study period. The time of the study is the first Special Observing Period (SOP-1) of FGGE, 5 January–4 March 1979.

The present study applies many of the techniques used by Chang and Lum (1985) to investigate the short term relationship between tropical heating and subtropical westerly maxima, but it is unique in a number of ways. First, we focus on the Southern Hemisphere, while Chang and Lum and many other studies were focused on the Northern Hemisphere. Second, we examine summertime subtropical westerly maxima, whereas nearly all prior studies have dealt with the wintertime hemisphere. Third, the average latitudinal distance between the tropical heat source (i.e., maxima upper-level divergence) and subtropical westerly maxima is much less in our study ($\sim$16°) than it is in the study of Chang and Lum ($\sim$24°) and most others. Nonetheless, in both studies the response occurs at about the same longitude as the heat source and appears to happen almost instantaneously (i.e., <12-h time lag). Finally, as noted earlier, the present investigation examines two regions of active tropical convection and their corresponding subtropical westerly wind maxima: the western Indian and the central Pacific oceans. The convective cloud band in the central Pacific, the SPCZ, is one of the most extensive and persistent features of the global-scale circulation pattern. To the best of our knowledge, there is little reference in the literature regarding the relationship between this region of active convection and its nearby subtropical westerly maximum.

2. Data and equations

As noted by Nogues-Paegle and Mo (1987) and Nogues-Paegle and Zhen (1987), any study which attempts to explain possible relationships between low-latitude heating and subtropical westerly maxima in terms of local Hadley-type circulations must be able to determine the divergent wind components reliably. Besides GLA, the two other major producers of FGGE gridded data sets were the Geophysical Fluid Dynamics Laboratory/NOAA at Princeton (GFDL) and the European Center for Medium-range Forecasts (ECMWF). Although the rotational wind components were similar among the three analyses, comparisons of the divergent wind components revealed much weaker divergent circulations in the ECMWF data than those of GFDL or GLA (Paegle et al. 1983, 1985). Paegle et al. (1983) discuss that this is probably the result of the initialization procedure, based on an adiabatic formulation, used by EMCWF. Therefore, we have chosen to use the GLA analyses in the present investigation.

The FGGE SOP-1 GLA analyses were derived from an assimilation cycle with the global fourth-order version of the GLA GCM described in detail by Kalnay-Rivas et al. (1977), Kalnay-Rivas and Hoitsma (1979), and more recently by Kalnay et al. (1983). The model is based on an energy-conserving scheme with all horizontal differences computed with fourth-order accuracy. Every two hours, a two-dimensional (latitude and longitude), 16th-order Shapiro (1970) filter is applied to sea level pressure, wind and potential temperature fields. There are nine vertical levels, equal in sigma, with a uniform nonstaggered horizontal grid of resolution 4° latitude by 5° longitude. A detailed description of analyzed and derived variables for the model is given by Baker (1983). Temporally, the data were originally analyzed during SOP-1 at four synoptic times, 0000, 0600, 1200, and 1800 UTC. However, a lack of 0600 UTC wind data from GOES-West, which strongly affected the upper-level divergence fields over the central Pacific Ocean, made it necessary to eliminate not only the 0600 UTC analyses, but also the 1800 UTC analyses in order not to bias the results with a diurnal influence. Therefore, the present study only utilizes the remaining 0000 and 1200 UTC analyses.

Most of the techniques applied in this study to examine the relationship between tropical heating and

higher latitude wind fields are commonly used in the literature and need not be discussed in detail. A few comments, however, are warranted.

One variable that is well correlated with tropical convective activity is velocity potential, since it indicates convergent and divergent flow. Consequently, it is relied upon heavily in the present investigation. As discussed by Hendon (1986), however, the use of velocity potential can be misleading because it represents the largest scale of the divergence. This can especially represent a problem when one is trying to quantify the spatial scale of a phenomenon, but this is not a goal of the present study. Our investigation is primarily concerned only with variations in the tropical velocity potential field to indicate changes in tropical heating. Moreover, the observed variations in velocity potential are in good agreement with fluctuations in other independent measurements (e.g., OLR, sea level pressure, lower and upper tropospheric divergence) of low latitude convective activity. Consequently, we feel the use of velocity potential can be extremely useful in studies of this nature.

Several authors have attempted to study the maintenance of subtropical jet streams through the conversion of divergent kinetic energy to rotational kinetic energy (Chen and Wiin-Nielsen 1976; Krishnamurti and Ramanthan 1982; Chen et al. 1988). We have also examined this conversion term using the open domain kinetic energy equations of rotational and divergent flow discussed by Chen et al. (1988). These equations can be written as

$$\frac{\partial k_D}{\partial t} \approx -\nabla\cdot(\vec{V}_D k) + (f+\zeta_R) \times (u_D v_R - u_R v_D) - \vec{V}_D\cdot\nabla\phi \quad (1)$$

$$\frac{\partial k_R}{\partial t} \approx -\nabla\cdot(\vec{V}_R k) - (f+\zeta_R) \times (u_D v_R - u_R v_D) - \vec{V}_R\cdot\nabla\phi \quad (2)$$

or, in symbolic notation

$$\frac{\partial k_D}{\partial t} \approx FD(k) - C(k_D k_R) + G(k_D)$$

$$\frac{\partial k_R}{\partial t} \approx FR(k) + C(k_D, k_R) + G(k_R).$$

The equations are approximate since only those terms important to the budgets of k_D and k_R have been retained. The notation used in Eqs. (1) and (2) is conventional. Subscripts D and R represent the divergent and rotational circulations, respectively, $FD(k)$ and $FR(k)$ represent the divergence of the horizontal kinetic energy fluxes, $G(k_D)$ and $G(k_R)$ represent the generation of kinetic energy by ageostrophic flow, and positive values of $C(k_D, k_R)$ represent the conversion of divergent to rotational kinetic energy.

3. Results

As mentioned in the Introduction, two regions of active tropical convection and corresponding subtropical westerly wind maxima are being examined. One of these regions, the SPCZ, contains an intense convective cloud band. During SOP-1 the SPCZ was particularly active for the first 2–3 weeks. Subsequently, convective activity weakened considerably in the SPCZ and the main area of convection shifted westward to become part of the Australian monsoon circulation. Concomitant with the reduced activity in the SPCZ was an enhancement of convection in the western Indian Ocean which lasted 2–3 weeks. Other regions in the tropical Southern Hemisphere maintained about the same level of convective activity throughout SOP-1. These changes in convection are clearly shown in the time-averaged OLR maps in Paegle et al. (1983) (their Fig. 10) for the periods 10–23 January 1979 and 26 January–7 February 1979. Since we do not possess adequate daily OLR data from February 1979 to construct similar diagrams, we can only give evidence of these changes in the monthly mean distributions of OLR for January (Fig. 1a) and February (Fig. 1b) 1979. The relevant point is that the patterns evident in Fig. 1 are in excellent agreement with those in Paegle et al. (1983). Areas with values of OLR ≤ 225 W m^{-2} are shaded in Fig. 1 and most likely contain active tropical convection (Heddinghaus and Krueger 1981). Note that the regions of maximum convective activity lie between the equator and 20°S, except for the SPCZ and the South Atlantic Convergence Zone (SACZ).

Upon close examination of the daily velocity potential fields, as well as distributions of the available daily OLR data and other variables, we found that the most persistent period of convective activity in the SPCZ occurred from early January until about 20 January. In contrast, the primary convective activity in the Indian Ocean existed from late January until slightly past the middle of February. Consequently, we decided to time average the analyses over two 15-day periods. The first period, 6–20 January, corresponded to strong convection in the SPCZ and weak activity in the western Indian Ocean, while the second period, 3–17 February, corresponded to the reverse of this pattern. In section 3a we examine a sample of time-averaged results which illustrate the relationship between tropical heating and subtropical wind maxima. Then, in section 3b, we investigate the daily variability of selected variables for all of SOP-1, which further illustrates this relationship. Finally, in section 3c, we look at a case study which shows the relationship in more detail.

a. Mean state

One indicator of tropical heating is an area of low level convergence or, similarly, a center of low surface pressure. Figure 2 shows charts of mean sea level pressure for Period 1 (6–20 January 1979), Period 2

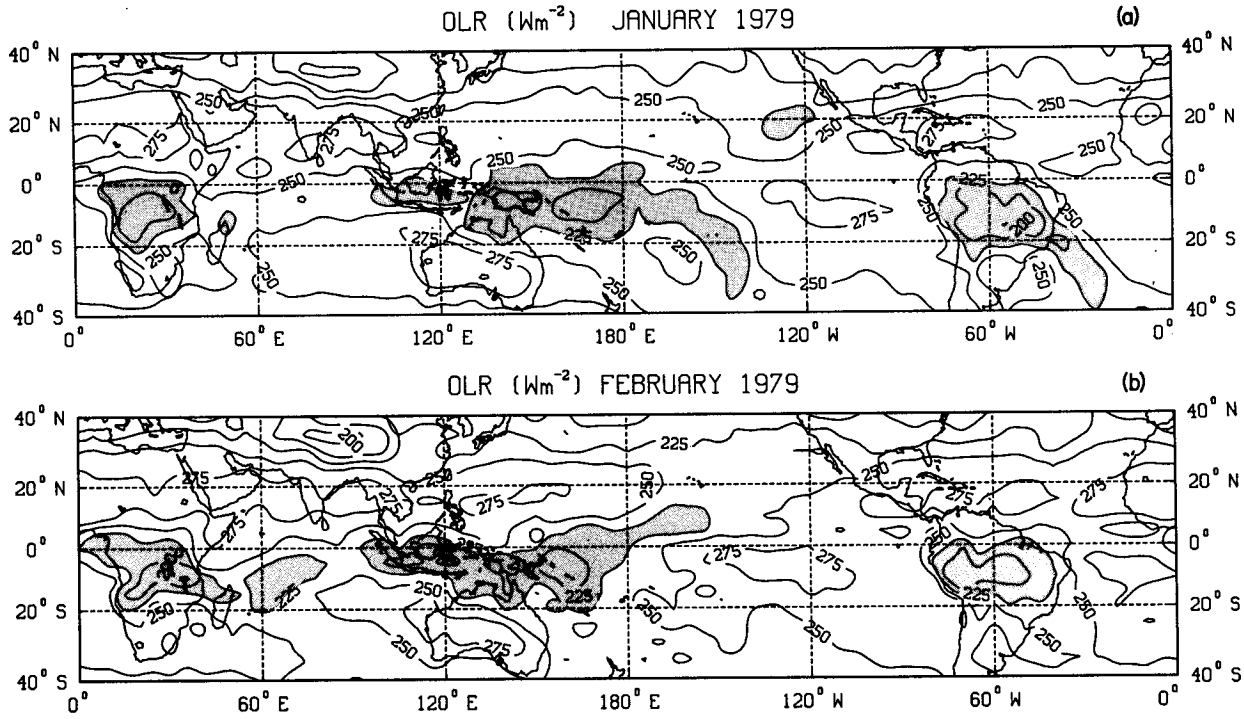

FIG. 1. Outgoing longwave radiation (OLR) in W m^{-2} for (a) January and (b) February 1979. Tropical areas with values of OLR $\leq$ 225 are shaded since they most likely contain active convection.

(3–17 February 1979), and their difference. In the Southern Hemisphere tropics and subtropics the most significant changes between Period 1 and Period 2 (Fig. 2c) were the increase in pressure in the SPCZ area and the decrease in the western Indian Ocean. There was also a smaller increase in pressure over Australia. As might be expected, the largest changes in pressure occurred in middle latitudes, particularly in the Northern Hemisphere; however, these circulation features are not within the focus of the present paper. More importantly, it should be appreciated that short-term time-mean pressure changes on the order of 4–8 mb in the tropics and subtropics, especially in summer, are quite significant.

Another indicator of convective activity and tropical heating is upper tropospheric divergence. Here we use velocity potential, χ, in the 250–200 mb layer to infer regions of divergence and convergence. Figure 3a shows a very large area of strong outflow associated with the SPCZ in Period 1. There is also a smaller area of weaker outflow associated with the SACZ. In contrast, upper level convergence is evident over the Indian Ocean. In Period 2 (Fig. 3b), as with other variables, the main changes in the Southern Hemisphere tropics took place over the South Pacific and Indian oceans. These changes, which consisted of large increases in upper level convergence over the SPCZ and divergence over the western Indian Ocean, are easily identified on the difference map of χ in Fig. 3c. A more modest increase in upper level convergence was observed during Period 2 over the SACZ, while over the western Pacific, the maximum divergence shifted to just east of New Guinea. Furthermore, the regions of upper level outflow are in good agreement with the areas containing low values of OLR (Fig. 1).

The relationship between tropical heat sources and subtropical westerly maxima can be seen by comparing the maps of the zonal wind component, u, in Fig. 4 to the heating as indicated by Figs. 1 and 3. In Period 1, Fig. 4a shows that the region of maximum westerly flow in the Southern Hemisphere subtropics is located over the South Pacific Ocean and is centered just north of 30°S and east of the IDL. There is also a subtropical westerly maximum oriented from southwest to northeast across South America and a band of strong westerlies near the equator over the eastern Pacific Ocean. In Period 2 (Fig. 4b), some significant changes took place, namely, the South Pacific westerlies decreased substantially and a westerly maximum developed over the Indian Ocean, just north of 30°S. Again, this is most easily seen on the difference map of u in Fig. 4c. In addition, a zonal wind acceleration of 15 m s^{-1} is evident between Australia and New Zealand, and the strong westerlies over the eastern Pacific weakened by 25 m s^{-1} near 90°W just south of the equator. Over South America, the westerly maximum oriented diagonally in Period 1 shifted to a more zonal position in Period 2, resulting in a westerly decrease of 15 m s^{-1}

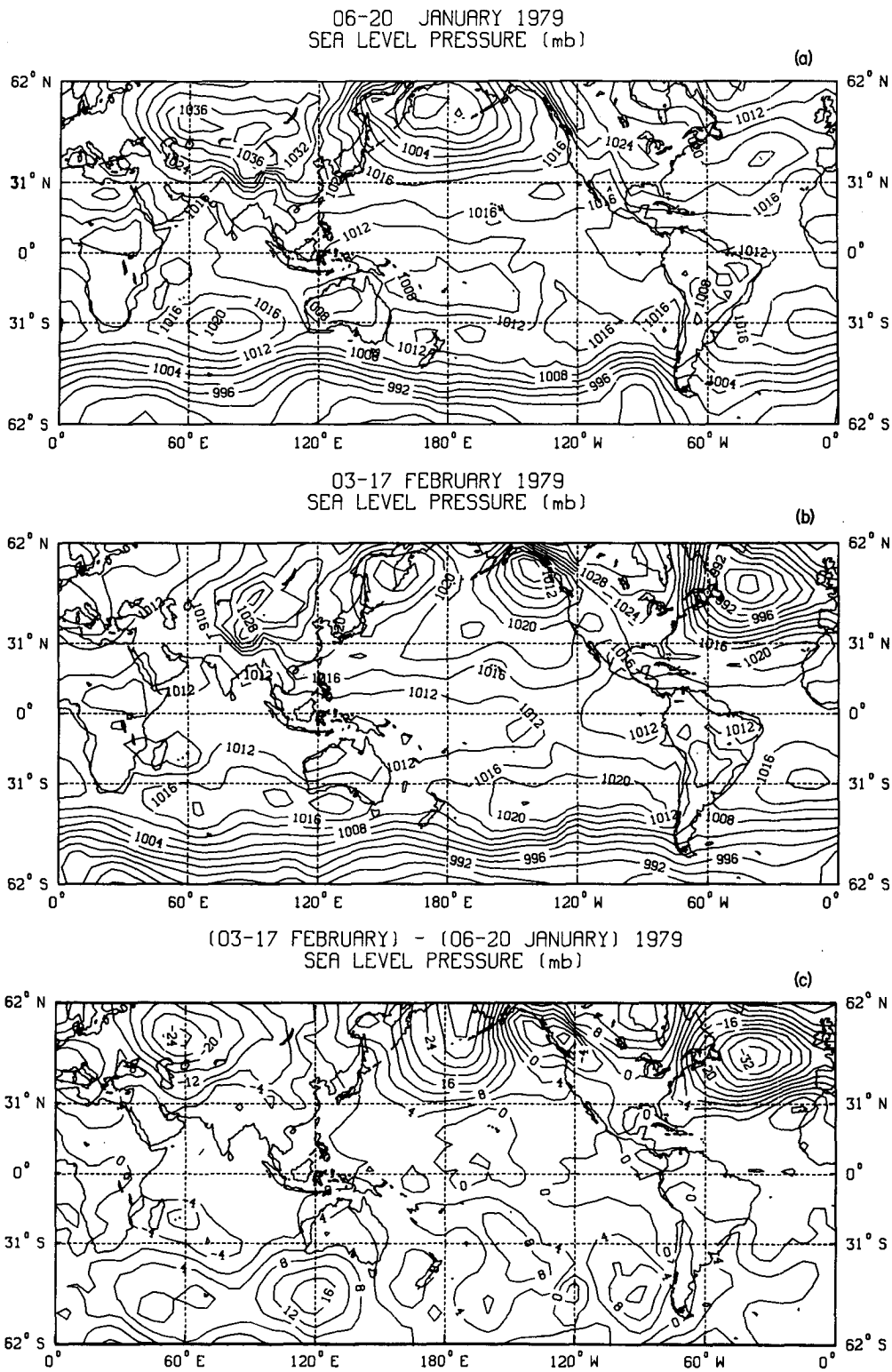

FIG. 2. Mean sea level pressure in millibars for (a) 6–20 January, (b) 3–17 February 1979, and (c) their difference.

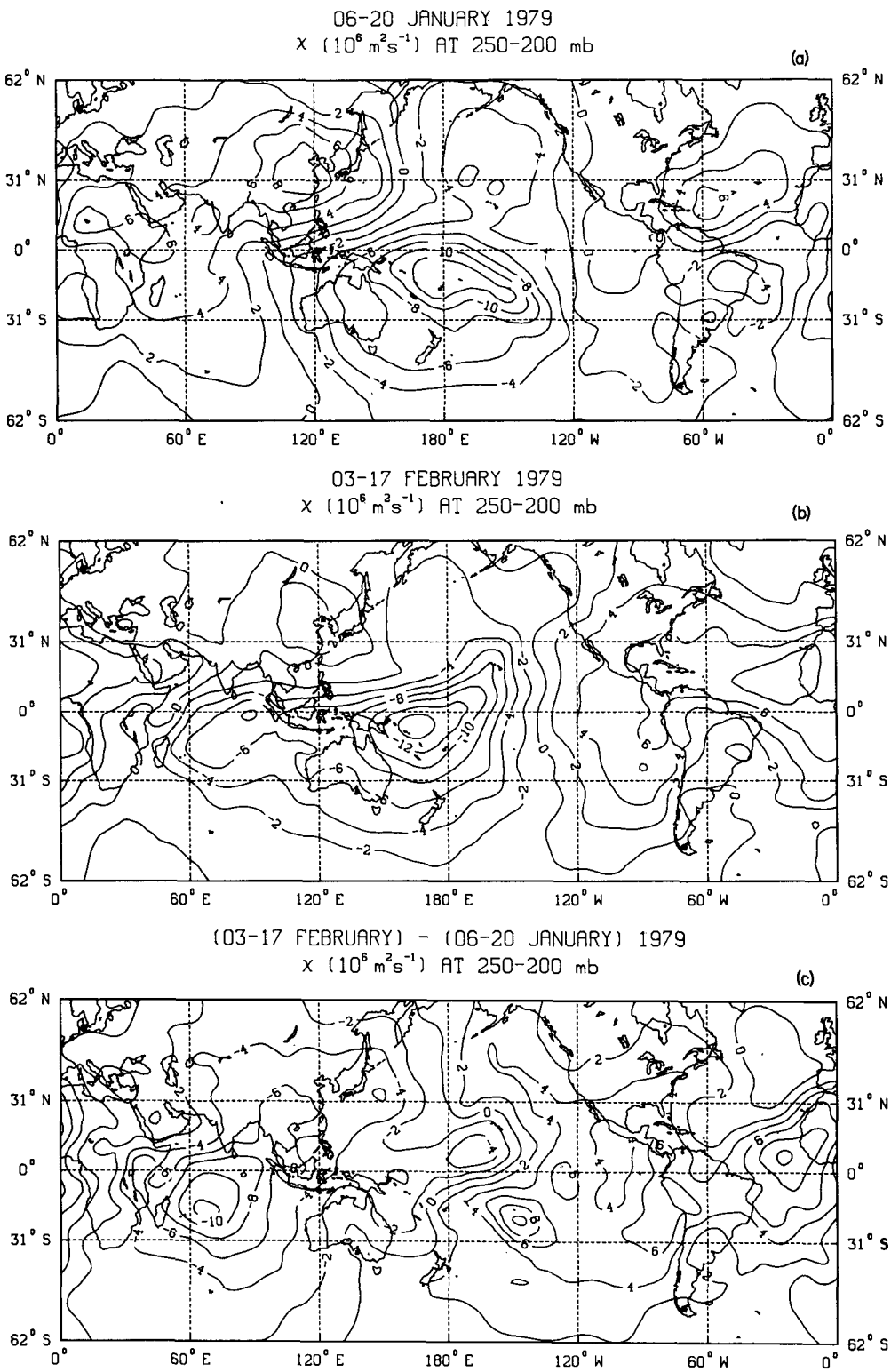

FIG. 3. As in Fig. 2, except for velocity potential in 10^6 m^2 s^{-1} in the 250–200 mb layer.

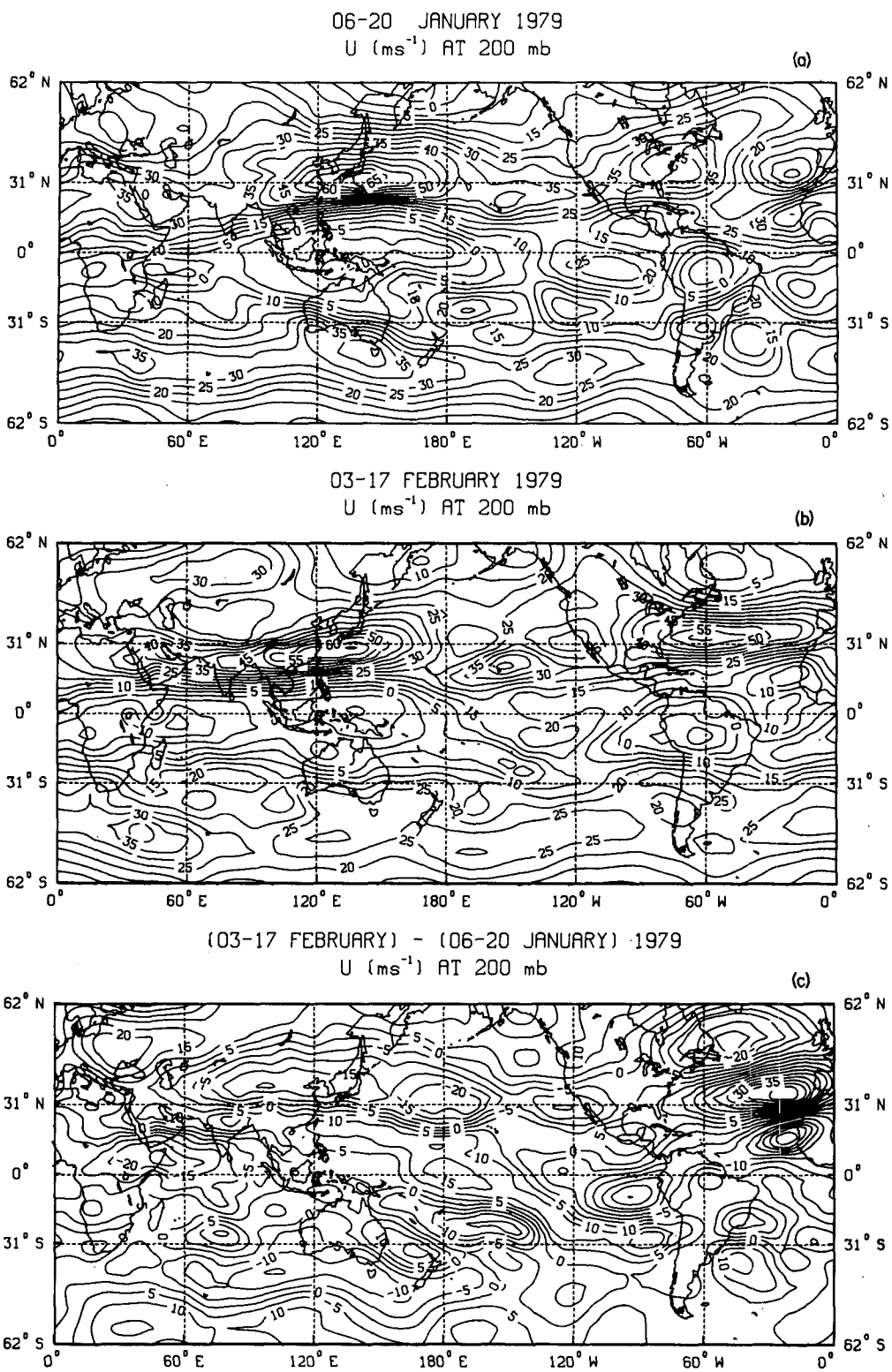

FIG. 4. As in Fig. 2, except for zonal wind component in m s^{-1} at 200 mb.

centered over the coast of Brazil with a corresponding increase just to the south. Also, it is seen that the higher latitude jet stream in the Southern Hemisphere is distinctly separate from the aforementioned subtropical wind maxima. Comparing the patterns in Figs. 1 and 3 to those in Fig. 4, it is seen that tropical heating and outflow aloft tend to be a maximum to the north of the respective subtropical westerly wind maxima. This is especially evident over the South Pacific and Indian oceans. This apparent correspondence will be examined in more detail in the following sections.

b. *Daily variability*

We now present the day-to-day fluctuations of three variables which relate tropical heat sources to subtropical wind distributions. They are displayed in the form of Hovmoeller diagrams in Figs. 5–7. The time span of each diagram is all of SOP-1, FGGE (i.e., 5 January–4 March 1979), while the longitudinal dimension extends from 20°E to 100°W. This allows us to focus on the South Pacific and Indian Ocean regions, where the greatest changes were observed in the mean state results. In Fig. 5a, velocity potential, χ, is shown for the 250–200 mb layer. It has been averaged between 2°S and 18°S since the upper tropospheric outflow which has been generated by heating is generally contained within these latitudes. The panel shows that maximum outflow is centered near the IDL from the beginning of the period to about 21 January, after which there is a weakening of the outflow for several days. In late January there is a resurgence of the outflow in the South Pacific which lasts until the end of the period, but it is now centered west of the IDL. During the first episode of strong outflow, there appears to be a slow eastward drift of the area containing maximum values, whereas during the second episode a slow westward progression is apparent. Perhaps the heating which is responsible for the outflow patterns is due to two different modes of wave motion. The panel of χ also shows a secondary region of maximum outflow over the Indian Ocean which is most active from about 27 January to 18 February. It appears that there were four episodes of stronger divergence during this period, each lasting only a few days. Note that the time-averaged results presented in section 3a were compiled for the latter three episodes, as well as for the first episode over the South Pacific.

The relationship between the upper tropospheric patterns of velocity potential in the tropics and the westerly winds in the subtropics is shown in Fig. 5b. This panel illustrates the superposition of outflow maxima on the 200 mb zonal wind component which has been averaged between latitudes, 18°S and 34°S. In this manner, it contains the subtropical westerly maxima of interest. Values of $u \geq 20$ m s^{-1} have been shaded and it is seen that westerly wind maxima correspond favorably to the pattern of tropical outflow. Moreover, it appears that many of the individual westerly maxima propagate eastward. A similar relationship was found by Chang and Lum (1985) in their paper where they examined tropical heating and subtropical jet streaks in the Northern Hemisphere during the winter season.

The results discussed thus far have established that tropical heating and its upper level outflow occur in conjunction with increases in subtropical westerly maxima located at similar longitudes but roughly 16° latitude farther south. Because of the latitudinal averaging, however, Fig. 5a can only indicate the east–west extent of the outflow. What remains to be shown is that the upper tropospheric outflow has a meridional component which is directed from the tropical source to the subtropical meridional locale. Figure 6a, which displays the north–south component of χ (i.e., v_χ) in the 250–200 mb layer, illustrates this connection. This variable has been averaged between 14°S and 22°S and values ≤ -2 m s^{-1} have been shaded to highlight regions of maximum poleward-moving air. It is seen that shaded areas of v_χ correspond favorably to shaded areas of χ, thus we conclude that a significant portion of the tropical outflow is directed southward into the region of the subtropical westerly maxima.

Let us now examine the relationship between v_χ and the zonal wind component. This is shown in Fig. 6b, and it is seen that the westerly maxima tend to form and propagate eastward away from regions containing maximum negative values of v_χ. Again, this result agrees favorably with the northern winter study of Chang and Lum (1985), and suggests that the tropical divergence may help force the strengthening of the subtropical jets by increasing v_χ within the upper branch of the local Hadley circulation.

Another way to investigate the tropical divergent circulations and the subtropical westerlies is through the kinetic energy equations for the divergent and rotational components of the flow. Specifically, the interaction between the divergent circulation and the rotational flow (i.e., subtropical westerly wind maxima) is represented by the conversion term, $C(k_D, k_R)$. This term is illustrated in Fig. 7a, and it has been averaged between the latitudes which contain the subtropical westerly maxima over the South Pacific and Indian oceans, 18°S to 34°S. Clearly, maximum positive values are in excellent spatial and temporal agreement with the subtropical wind maxima illustrated in Figs. 5b and 6b. Furthermore, our analyses of the remaining terms in Eq. (2) showed that although $G(k_R)$ and $FR(k)$ were the dominant contributors to the maintenance of k_R at higher latitudes (especially in the Northern Hemisphere), $C(k_D, k_R)$ was dominant in the latitudes of interest to the present investigation. Moreover, Fig. 7b illustrates that local values of $G(k_D)$ and $C(k_D, k_R)$ are comparable in magnitude, and the patterns of their distribution are similar. Since $FD(k)$ (not shown) is small, and compared to k_R the divergent kinetic energy (k_D) is small, we conclude that the generated di-

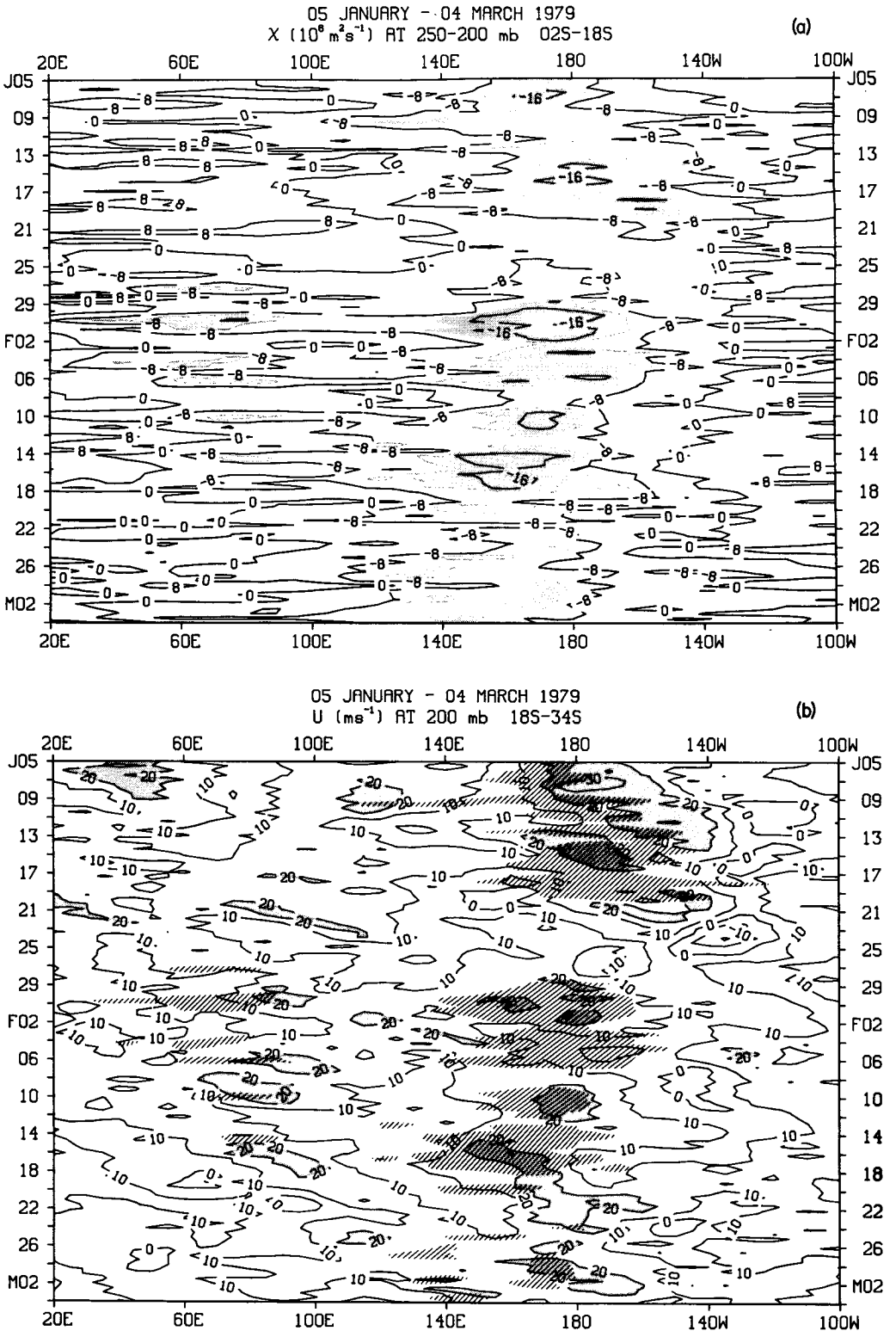

FIG. 5. Hovmoeller diagrams of (a) velocity potential (10^6 m^2 s^{-1}) in the 250–200 mb layer, and (b) zonal wind component (m s^{-1}) at 200 mb for 5 January–4 March 1979. Values of $\chi \leq -12$ and $u \geq 20$ are shaded, and in (b) $\chi \leq -12$ is indicated by hatching.

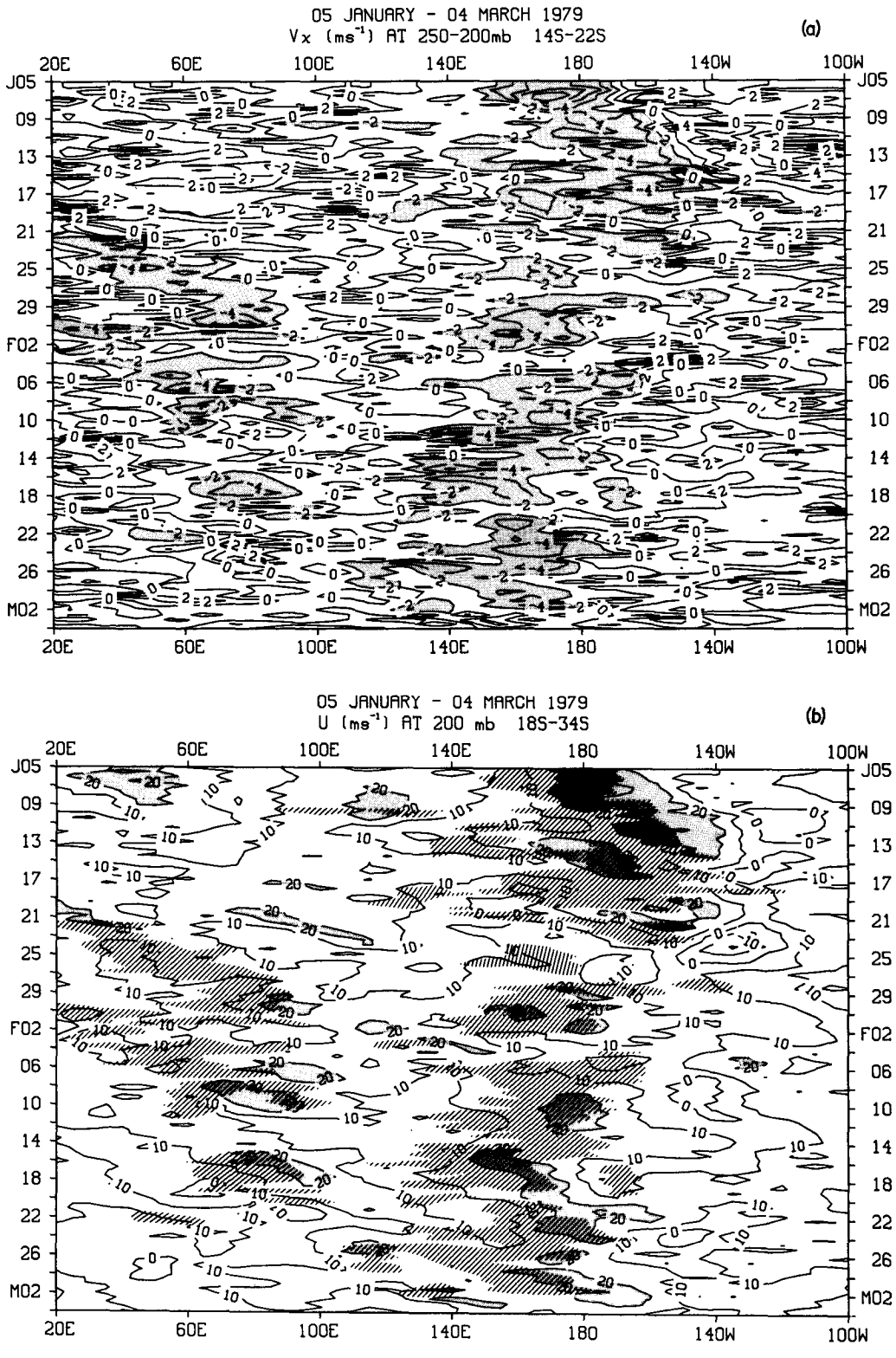

FIG. 6. Hovmoeller diagrams of (a) meridional component of χ (m s^{-1}) in the 250–200 mb layer, and (b) zonal wind component (m s^{-1}) at 200 mb for 5 January–4 March 1979. Values of $v_x \leq -2$ and $u \geq 20$ are shaded, and in (b) $v_x \leq -2$ is indicated by hatching.

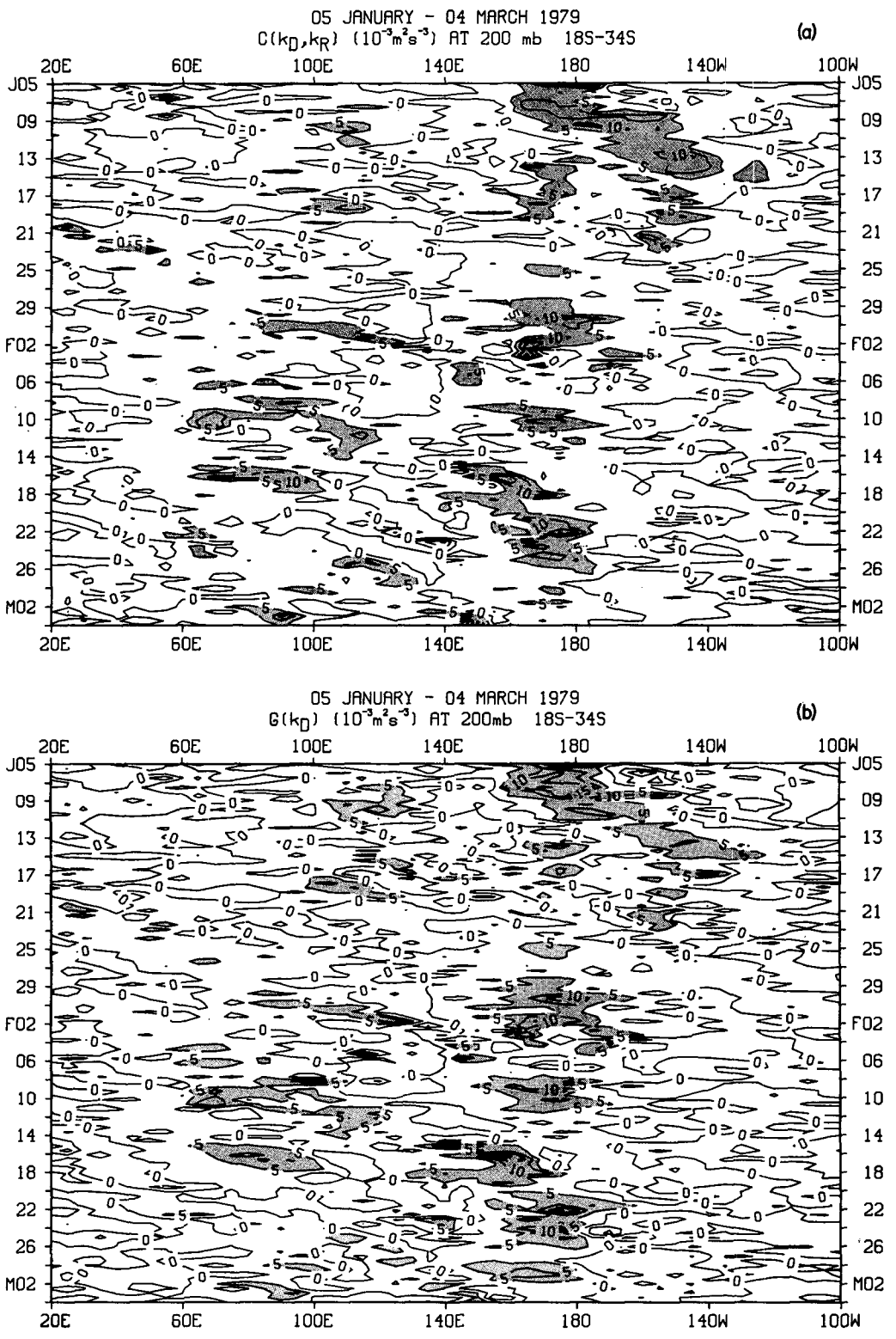

FIG. 7. Hovmoeller diagrams of (a) conversion of divergent to rotational kinetic energy (10^{-3} m^2 s^{-3}), and (b) generation of divergent kinetic energy (10^{-3} m^2 s^{-3}) at 200 mb for 5 January–4 March 1979. Values of $C(k_D, k_R) \geq 5$ and $G(k_D) \geq 5$ are shaded.

vergent kinetic energy is mostly converted to support the rotational flow in the regions of the subtropical westerly maxima. These results are in good agreement with those of Chen et al. (1988) in a study on the maintenance of the winter subtropical jet streams in the Northern Hemisphere.

A quantitative evaluation of the time-lag correlation at the same longitudes between upper tropospheric velocity potential in the tropics and westerly winds in the subtropics is shown in Fig. 8. The latitudinal averaging for both χ and u is the same as in Fig. 5, and the time period represented is all of SOP-1. The values shown in Fig. 8 are simple correlation coefficients with shaded (hatched) values of $R \geq 0.3$ ($R \leq -0.3$) having a significance level > 99%. It is seen that the highest positive correlations occur over four distinct areas; the Indian Ocean between 70°E and 85°E; the western Pacific near 150°E; the central Pacific in the vicinity of the SPCZ; and a narrow band near the SACZ. The reason for the lower correlations over the western Indian Ocean relative to those over the western and central Pacific can be explained by noting in Fig. 5 the presence of isolated wind maxima within this region in mid-January, a time period in which the χ field exhibited upper-level convergence. In addition, even though they represent only a portion of SOP-1, the difference maps in Figs. 3 and 4 show that the greatest change in χ was located approximately 5°–10° of longitude west of the most significant increase in the zonal winds. Similarly, these same figures support the high correlations found on either side of the IDL. In the SPCZ region, decreases in convection after mid-January clearly correspond to decreases in the subtropical westerlies, while the inverse applies in the western Pacific. Between 30°W and 45°W, the narrow band of positive correlations is related to decreases in both divergence and the westerly maxima over the coast of Brazil. Also, it is interesting to note the negative correlations exhibited over the eastern portions of the Pacific and Atlantic oceans. In both regions, these correlations were the result of a strengthening with time of already existing upper-level convergence while isolated weak westerly wind maxima passed through the subtropics. In general, our examination of Hovmoeller diagrams for the region bounded by 100°W and 20°E (i.e., the eastern Pacific and the Atlantic) showed no apparent correlation between areas of upper tropospheric tropical divergence and subtropical wind maxima, with the exception of the diagonal extension of the SACZ over the coast of Brazil.

Figure 8 also illustrates that the most significant correlations occur at zero time lag and are more or less symmetric about the zero lag line, which suggests that any cause/effect relationship between tropical heating and subtropical wind maxima takes place primarily in less than 12 hours (i.e., the temporal spacing of the data). Finally, as Chang and Lum (1985) discuss, while correlations on the order of 0.3 to 0.4 seem weak, one must remember that forcing mechanisms other than tropical divergence undoubtedly contribute to the day-to-day changes of subtropical winds. With this in mind, plus the fact that we are examining the summer hemisphere where the Hadley circulation is much weaker than in the winter hemisphere, it is clear that these positive correlations result from several periods of significant, nearly simultaneous enhancements of both tropical divergence and subtropical winds.

In order to examine the relationship between tropical heating and subtropical westerly maxima in more detail for the SPCZ and Indian Ocean regions, we now show a time series of χ vs. u for each region. Figure 9 depicts the time plot of area-averaged values of both variables for the SPCZ for the entire period of SOP-1. The variables have been averaged from 170°W to 140°W since these longitudes contained some of the highest positive correlation coefficients in Fig. 8. As can be seen, the best agreement between the two curves occurs in January, with the largest values from early in the period to about 20 January. The worst agreement is after 10 February when the tropical heating has shifted westward away from the SPCZ area. Figure 10 depicts the same two variables for the Indian Ocean region. Again,

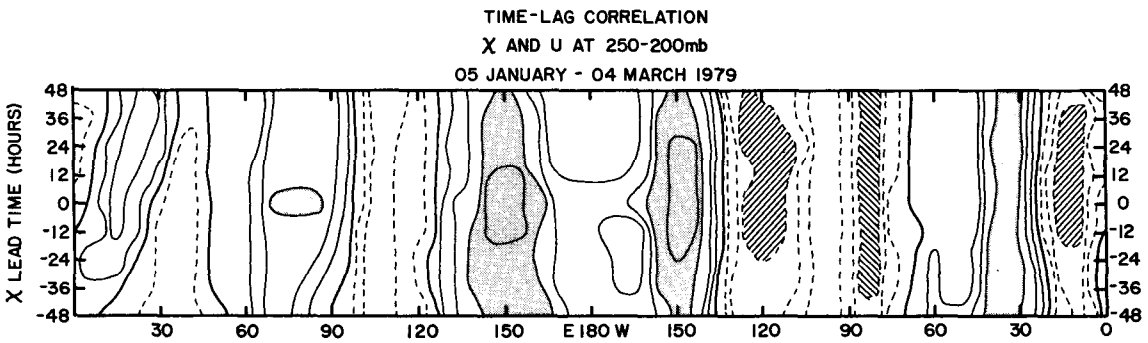

FIG. 8. Time-lag correlation coefficients (R) between 250–200 mb velocity potential, averaged over 2°–18°S, and 200 mb zonal wind, averaged over 18°–34°S, at the same longitude for SOP-1. Isopleth interval is 0.1. Areas enclosed by $R \geq 0.3$ (significant levels ≥ 99%) are shaded, and areas enclosed by $R \leq -0.3$ are hatched.

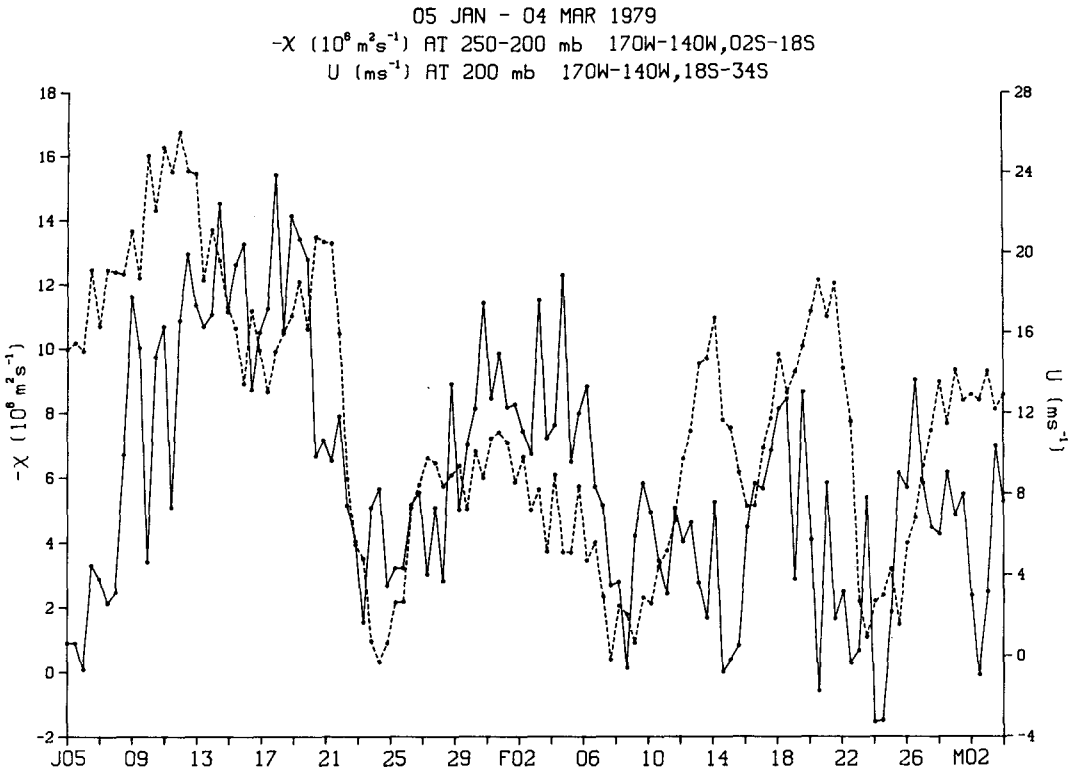

FIG. 9. Time series of velocity potential (10^6 m^2 s^{-1}) in the 250–200 mb layer, averaged over 2°–18°S, 170°–140°W (solid) and zonal wind component (m s^{-1}) at 200 mb, averaged over 18°–34°S, 170°–140°W (dashed) for 5 January–4 March 1979.

the longitudes over which the area averages were computed contained the highest correlation coefficients. As mentioned earlier, a very poor correlation between variables is evident until near the end of January and, again, toward the end of the period. From the end of January until about 18 February, however, a good agreement is seen. Note that the period of good agreement exists only when upper level outflow occurs.

c. *Case study*

There were several examples from which to choose a case study that illustrates the relationship between a source of tropical heating and a corresponding subtropical westerly maximum. The case study we selected occurred in the SPCZ region during a period when a cyclone developed in the tropics and subsequently moved toward middle latitudes. In a previous paper, one of the authors (Vincent 1985) discussed the details of this cyclone event. He noted that a westerly maximum was present aloft, to the south and east of the surface cyclone, and that it propagated southward and eastward along a track which the cyclone followed about one day later.

Figure 11 shows the upper tropospheric patterns of velocity potential and zonal wind for the main portion of the cyclone's life cycle. The location of the cyclone is indicated by L. At the first time shown, 0000 UTC 13 January (Fig. 11a), maximum outflow is seen to occur near 22°S, 150°W. This is the approximate location of the surface cyclone, which is in its developing stage. There is a maximum in the westerly wind at about 26°S, 145°W, which we believe is related to the cyclone's heating field. By 0000 UTC 14 January (Fig. 11b), very little change has occurred in the pattern of either variable. Twelve hours later, however, changes have taken place. Figure 11c, valid at 1200 UTC 14 January, shows that the wind maximum has moved to 30°S, 140°W. At this time, the cyclone was fully developed, but had not yet begun to propagate toward middle latitudes. It is seen that the upper level outflow is very strong, but that the location of its maximum value has moved only slightly from the previous time. By 0000 UTC 15 January, the cyclone had begun to move poleward and eastward. This fact is reflected in the pattern of velocity potential which shows maximum outflow near 26°S, 145°W (Fig. 11d). Correspondingly, the westerly maximum has propagated southeastward and, at this time, is located near 34°S, 135°W. Finally, at 1200 UTC 15 January, Fig. 11e indicates a further propagation toward the southeast of maxima in outflow and westerly wind. By 0000 UTC 16 January (not shown), the cyclone was beginning to decay and was located at approximately 35°S, 140°W, and the westerly maximum streak had exited the analysis area.

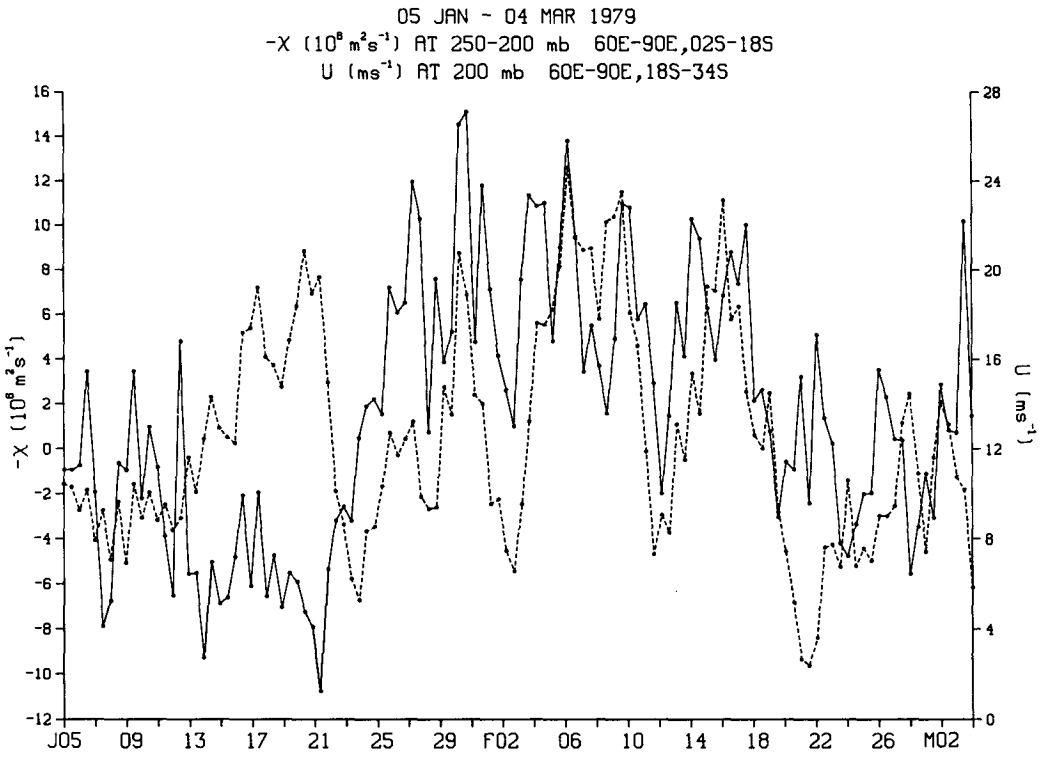

FIG. 10. As in Fig. 9, except averaged over 60°–90°E.

4. Concluding remarks

Over the past decade numerous investigators have used both observational and modeling data to study the link between tropical heating and higher latitude circulations and, specifically, westerly wind maxima. The large majority of these studies, however, have focused on Northern Hemisphere circulations. Studies of Southern Hemisphere interactions have been less frequent, although aided substantially by the FGGE special observing system. Nonetheless, to our knowledge, nearly all of this research has focused on circulations in the winter hemisphere.

The purpose of the present investigation has been to examine the short-term relationship between the upper level outflow from tropical heat sources and subtropical westerly maxima in the Southern Hemisphere during summer, namely, SOP-1 FGGE. Like many of the winter hemisphere studies, we found that episodes of strong outflow, measured by upper tropospheric velocity potential, were well correlated with the enhancement and propagation of subtropical westerly maxima located at similar longitudes. Energetically, this was manifested as a strong conversion of divergent to rotational kinetic energy in the regions of the maximum westerlies. This relationship was particularly evident in the South Pacific during January and in the Indian Ocean during February. Over the eastern Pacific and Atlantic oceans, no significant positive correlations were found to exist, with the exception of the southeastward extension of the SACZ and its corresponding westerly maximum over the coast of Brazil. In general, very poor correlations between tropical velocity potential and subtropical zonal winds were noted at all longitudes when upper level convergence was present (e.g., Fig. 10 during early to mid-January). This would indicate that subtropical westerly maxima can exist at all times, but are particularly enhanced during periods of strong upper level tropical outflow.

Another finding of this study was that the latitudinal distance between the maximum tropical outflow regions and the subtropical westerly flows was, in the mean, about 16°, compared to 25° to 35° in most other studies. In agreement, however, was that the westerly maxima were usually slightly east of their corresponding tropical heat sources. Because of the short distance between these phenomena, it is difficult to conclude what the response time is from our 12-h data. Our analyses seem to suggest that it is less than 12 h. Consequently, no definite conclusion about a cause/effect relationship can be made. In fact, for the South Pacific cyclone case discussed, where the average distance between the heat source and wind maxima was much less than 16° and both features propagated southeastward, it is possible that the baroclinic zone set up by the wind maximum was responsible for enhancing the cyclone's heating field (Trenberth 1976; Robertson et al. 1989). In other words, the upper tropospheric wind maximum might have led, rather than trailed, the upper level outflow. On the other hand, our

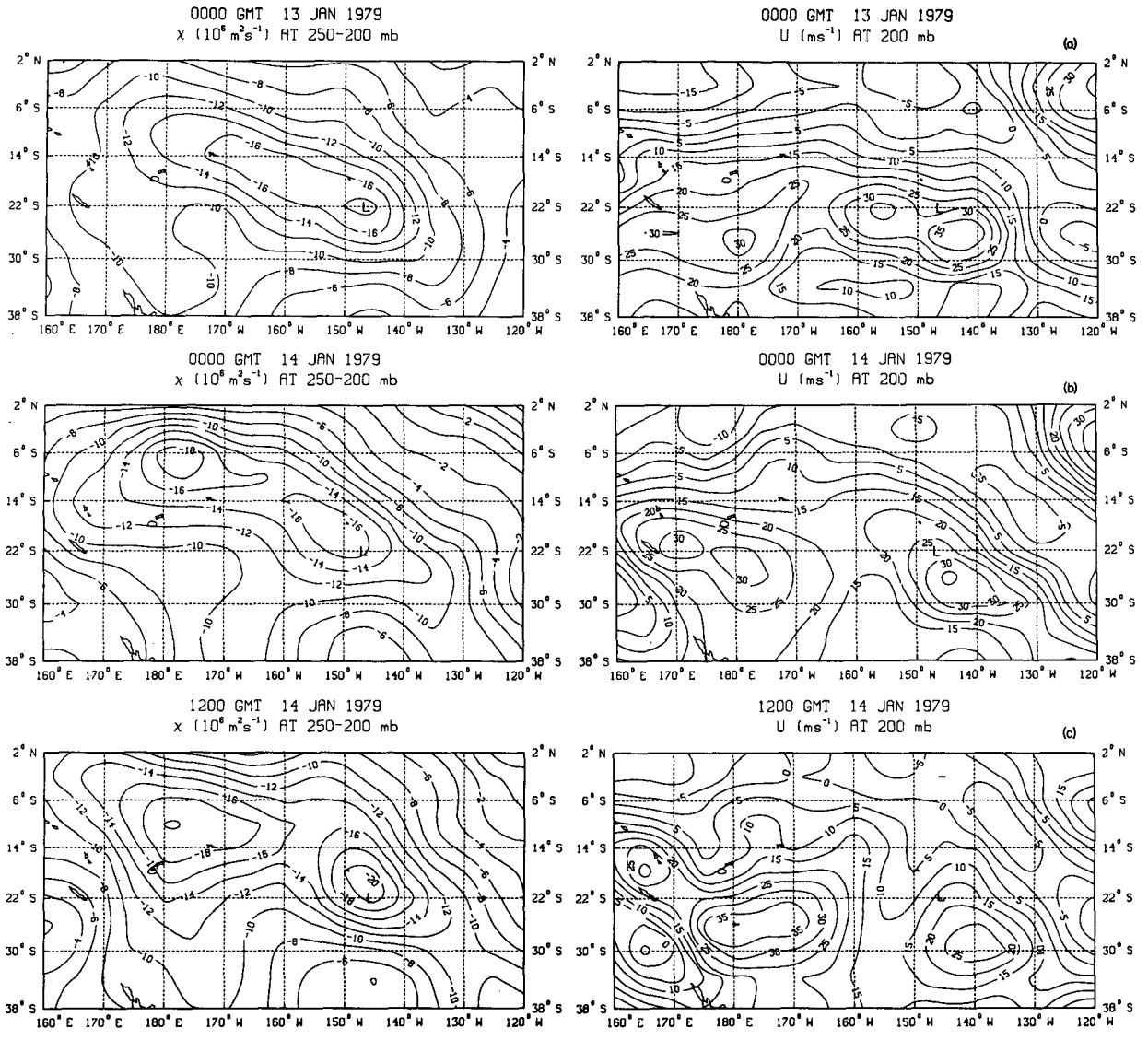

FIG. 11. Velocity potential (10^6 m^2 s^{-1}) in the 250–200 mb layer and zonal wind component (m s^{-1}) at 200 mb for (a) 0000 UTC 13 January, (b) 0000 UTC 14 January, (c) 1200 UTC 14 January, (d) 0000 UTC 15 January and (e) 1200 UTC 15 January 1979. An L indicates the center of the surface low pressure area.

recent unpublished analysis of localized Eliassen–Palm flux diagnostics (using the formulation by Trenberth 1986) for the South Pacific during 6–20 January revealed that the impact of the cyclones propagating along the SPCZ was to accelerate the time-mean subtropical westerlies on the poleward side of the cloud band between 170°W and 140°W. Evidently, a complicated two-way interaction between the heating and wind fields in the SPCZ region is likely.

Finally, it has occurred to us that the reason for strong tropical heating in the SPCZ during 6–20 January and the Indian Ocean during 3–17 February might be due to some type of periodic oscillation. For instance, we may have captured a major part of the heating signal associated with the 30–50 day wave oscillation in the tropics in our temporal averaging. It is well known in the literature that the 30–50 day oscillation was present throughout the FGGE year. Lorenc (1984) used FGGE ECMWF Level III-b data to examine the 200 mb velocity potential field and found a clear signal in the entire FGGE period of an eastward propagating wave with zonal wavenumber 1 and a period of 30–50 days. Krishnamurti et al. (1985) also studied the divergent circulations during the FGGE year with 30–50 day filtered EMCWF data. Their results show a planetary-scale divergence wave that traverses around the globe eastward at a rate of approximately 8° longitude per day. This periodicity is compatible with our results since the SPCZ was convectively active in early to mid-January, whereas the western Indian Ocean, which showed suppressed convection at this time, became active in early February. Moreover,

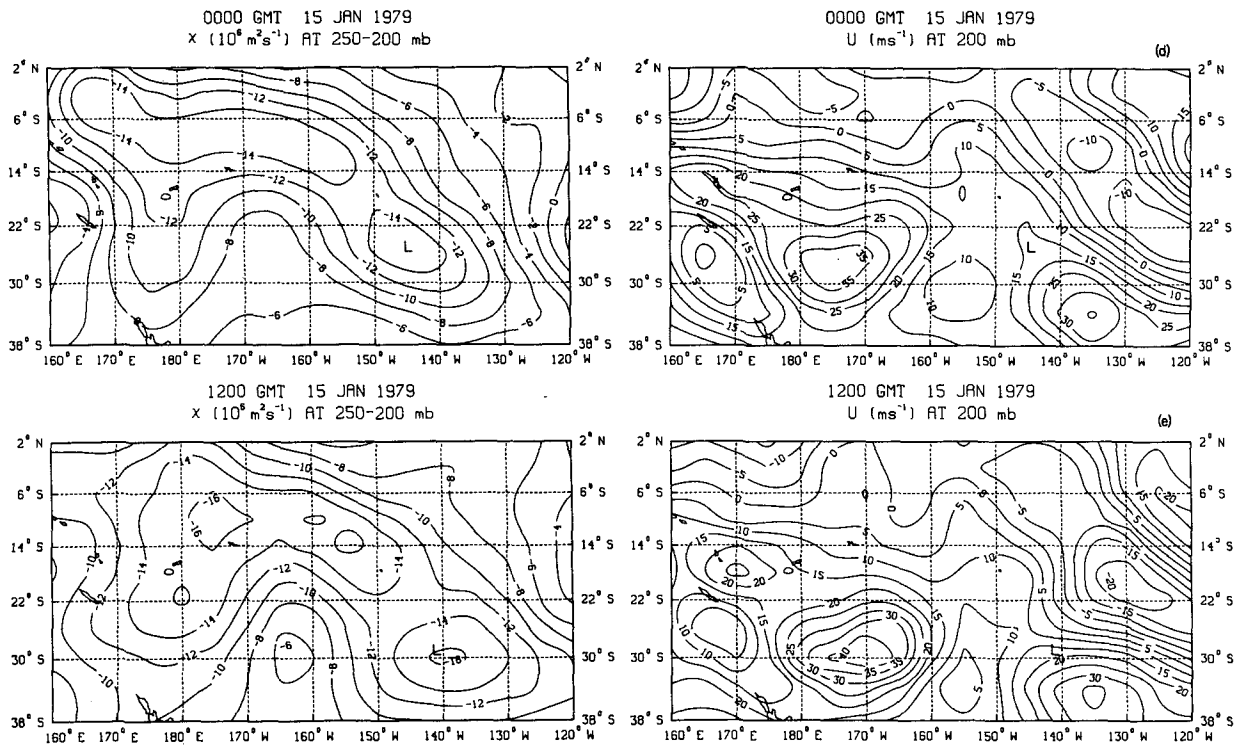

FIG. 11. (*Continued*)

this result is in good agreement with the OLR anomaly studies of Murakami and Nakazawa (1985), Murakami et al. (1986) and Weickmann et al. (1985) discussed previously. All of these investigations concluded that the strongest convection anomalies associated with the 30–50 day oscillation are confined to the Indian Ocean and western Pacific equatorial sectors, and that the convection in the SPCZ region is out of phase with that in the Indian Ocean. Although this is in good agreement with our mean state results, however, Fig. 5a clearly shows a westward progression of maximum outflow over the western Pacific throughout February. Perhaps the 30–50 day oscillation did influence our results, but is not evident since we neither time-filtered our data nor examined any type of anomaly fields.

Another possibility of a periodic oscillation which might have played an important role during the present study is the 2–3 month cycle discussed by Lau and Chan (1983a,b). They suggest that the tropical diabatic heat sources and sinks appear to exhibit a dipole-like oscillation which alternates between dry and wet periods over the equatorial central Pacific and the maritime continent of Indonesia. They state that February 1979 was characteristic of a wet period, which consists of strong convection over the central Pacific, an eastward migration of the SPCZ, and an equatorial migration of the ITCZ over the central and eastern Pacific, resulting in considerable shrinkage of the eastern Pacific dry zone. Our results do not show such a pattern for February. In fact, this description is more characteristic of our January pattern. In contrast to the finding of Lau and Chan, our February results correspond more to their definition of a dry period, which consists of intense convection over the maritime continent and an extensive eastern Pacific dry zone.

Acknowledgments. The authors sincerely appreciate the help from the two anonymous reviewers whose suggestions and comments greatly improved the paper. Also, thanks to Dr. William Lau (GSFC/NASA) for providing the OLR data and Ms. Helen Henry for typing the manuscript. In addition, they gratefully acknowledge GSFC/NASA for providing the GLA analyses. This research was sponsored by the National Aeronautics and Space Administration under Contract NAS8-37127 issued to Dr. Dayton G. Vincent, Purdue University.

REFERENCES

Baker, W. E., 1983: Objective analysis and assimilation of observational data from FGGE. *Mon. Wea. Rev.*, **111**, 328–342.

Blackmon, M. L., J. M. Wallace, N. C. Lau and S. M. Mullen, 1977: An observational study of the Northern Hemisphere wintertime circulation. *J. Atmos. Sci.*, **34**, 1040–1053.

Chang, C.-P., and K. M. Lau, 1980: Northeasterly cold surges and near-equatorial disturbances over the winter MONEX area during December 1974. Part II: Planetary-scale aspects. *Mon. Wea. Rev.*, **108**, 298–312.

——, and ——, 1982: Short-term planetary-scale interactions over the tropics and midlatitudes during northern winter. Part I: Contrasts between active and inactive periods. *Mon. Wea. Rev.*, **110**, 933–946.

——, and K. G. Lum, 1985: Tropical–midlatitude interactions over Asia and the western Pacific Ocean during the 1983/84 northern winter. *Mon. Wea. Rev.*, **113,** 1345–1358.

Chelliah, M., J. E. Schemm and H. M. van den Dool, 1988: The impact of low-latitude anomalous forcing on local and remote circulation: Winters 1978/79–1986/87. *J. Climate,* **1,** 1138–1152.

Chen, T.-C., and A. Wiin-Nielsen, 1976: On the kinetic energy of the divergent and nondivergent flow in the atmosphere. *Tellus,* **28,** 486–498.

——, R.-Y. Tzeng and H. van Loon, 1988: A study on the maintenance of the winter subtropical jet streams in the Northern Hemisphere. *Tellus,* **40,** 392–397.

Gill, A. E., 1980: Some simple solutions for heat-induced tropical circulation. *Quart. J. Roy. Meteor. Soc.*, **106,** 447–462.

Heddinghaus, T. R., and A. F. Krueger, 1981: Annual and interannual variations in outgoing longwave radiation over the tropics. *Mon. Wea. Rev.*, **109,** 1208–1218.

Hendon, H. H., 1986: Streamfunction and velocity potential representation of equatorially trapped waves. *J. Atmos. Sci.*, **43,** 3038–3042.

Hoskins, B. J., and D. Karoly, 1981: The steady linear response of a spherical atmosphere to thermal and orographic forcing. *J. Atmos. Sci.*, **38,** 1179–1196.

Kalnay, E., R. Balgovind, W. Chao, D. Edelmann, J. Pfaendtner, L. Takacs and K. Takano, 1983: Documentation of the GLAS fourth order general circulation model. Vols. I, II, and III, NASA Tech. Memo 86064, Goddard Space Flight Center.

Kalnay-Rivas, E., and D. Hoitsma, 1979: The effect of accuracy, conservation and filtering on numerical weather forecasting. Preprints, *Fourth Conf. Numerical Weather Prediction,* Silver Springs, Amer. Meteor. Soc., 302–312.

——, A. Bayliss and J. Storch, 1977: The 4th order GISS model of the global atmosphere. *Beitr. Phys. Atmos.*, **50,** 299–311.

Knutson, T. R., K. M. Weickmann and J. E. Kutzbach, 1986: Global-scale intra-seasonal oscillations of outgoing longwave radiation and 250 mb zonal wind during Northern Hemisphere summer. *Mon. Wea. Rev.*, **114,** 605–623.

Krishnamurti, T. N., 1979: Tropical meteorology. *Compendium of Meteorology II,* WMO-No. 364, A. Wiin-Nielsen, Ed. World Meteorological Organization, 428 pp.

——, and Y. Ramanathan, 1982: Sensitivity of monsoon onset to differential heating. *J. Atmos. Sci.*, **39,** 1290–1306.

——, M. Kanamitau, W. J. Ross and J. D. Lee, 1973: Tropical east-west circulations during the northern winter. *J. Atmos. Sci.*, **30,** 780–787.

——, P. K. Jayakumar, J. Sheng, N. Surgi and A. Kumar, 1985: Divergent circulations on the 30–50 day time scale. *J. Atmos. Sci.* **42,** 364–375.

Lau, K.-M., and P. H. Chan, 1983a: Short-term climate variability and atmospheric teleconnection as inferred from outgoing longwave radiation. Part I: Simultaneous relationships. *J. Atmos. Sci.*, **40,** 2735–2750.

——, and ——, 1983b: Short-term climate variability and atmospheric teleconnection as inferred from outgoing longwave radiation. Part II: Lagged correlations. *J. Atmos. Sci.*, **40,** 2751–2767.

——, and H. Lim, 1984: On the dynamics of equatorial forcing of climate teleconnections. *J. Atmos. Sci.*, **41,** 161–176.

——, C.-P. Chang and P. H. Chan, 1983: Short-term planetary-scale interactions over the tropics and midlatitudes. Part II: Winter-MONEX period. *Mon. Wea. Rev.*, **111,** 1372–1388.

Lim, H., and C.-P. Chang, 1983: Dynamics of teleconnections and Walker circulations forced by equatorial heating. *J. Atmos. Sci.*, **40,** 1897–1915.

Lorenc, A. C., 1984: The evolution of planetary scale 200 mb divergence flow during the FGGE year. *Quart. J. Roy. Meteor. Soc.*, **110,** 427–441.

Madden, R., and P. Julian, 1971: Detection of a 40–50 day oscillation in the zonal wind. *J. Atmos. Sci.*, **28,** 702–708.

——, and ——, 1972: Description of global scale circulation cells in the tropics with a 40–50 day period. *J. Atmos. Sci.*, **29,** 1109–1123.

Murakami, T., and T. Nakazawa, 1985: Tropical 45 day oscillations during the 1979 Northern Hemisphere summer. *J. Atmos. Sci.*, **42,** 1107–1122.

——, L.-X. Chen, A. Xie and M. L. Shrestha, 1986: Eastward propagation of 30–60 day perturbations as revealed from outgoing longwave radiation data. *J. Atmos. Sci.*, **43,** 961–971.

Nogues-Paegle, J., and Z. Zhen, 1987: The Australian subtropical jet during the second observing period of the Global Weather Experiment. *J. Atmos. Sci.*, **44,** 2277–2289.

——, and K. C. Mo, 1987: Spring-to-summer transitions of global circulations during May–July 1979. *Mon. Wea. Rev.*, **115,** 2088–2102.

——, and ——, 1988: Transient response of the Southern Hemisphere subtropical jet to tropical forcing. *J. Atmos. Sci.*, **45,** 1493–1508.

Opsteegh, J. D., and H. M. van den Dool, 1980: Seasonal differences in the stationary response of a linearized PE-model: Prospects for long range weather forecasting? *J. Atmos. Sci.*, **37,** 2169–2185.

Paegle, J., J. N. Paegle and F. P. Lewis, 1983: Large-scale motions of the tropics in observations and theory. *Pure Appl. Geophys.*, **121,** 947–982.

Paegle, J. N., J. Paegle and Z. Zhao, 1985: Intercomparisons of 200 mb global wind field from level III-b data sets. GARP Special Rep. No. 44, of the Seminar on Progress in Tropical Meteorology as a Result of the Global Weather Experiment, Tallahassee, 20–35.

Palmen, E., and C. W. Newton, 1969: *Atmospheric Circulation Systems,* Academic Press, 603 pp.

Physick, W. L., 1981: Winter depression tracks and climatological jet streams in the Southern Hemisphere during the FGGE year. *Quart. J. Roy. Meteor. Soc.*, **107,** 883–898.

Robertson, F. R., D. G. Vincent and D. M. Kann, 1989: The role of diabatic heating in maintaining the upper-tropospheric baroclinic zone in the South Pacific. *Quart. J. Roy. Meteor. Soc.*, in press.

Sardeshmukh, P. D., and B. J. Hoskins, 1988: The generation of global rotational flow by steady idealized tropical divergence. *J. Atmos. Sci.*, **45,** 1228–1251.

Shapiro, R., 1970: Smoothing, filtering and boundary effects. *Rev. Geophys. Space Phys.*, **8,** 359–387.

Simmons, A. J., 1982: The forcing of stationary wave motion by tropical diabatic heating. *Quart. J. Roy. Meteor. Soc.*, **108,** 503–534.

Trenberth, K. E., 1976: Spatial and temporal variations of the Southern Oscillation. *Quart. J. Roy. Meteor. Soc.*, **102,** 639–653.

——, 1986: An assessment of the impact of transient eddies on the zonal flow during a blocking episode using localized Eliassen–Palm flux diagnostics. *J. Atmos. Sci.*, **43,** 2070–2087.

Vincent, D. G., 1985: Cyclone development in the South Pacific convergence zone during FGGE, 10–17 January 1979. *Quart. J. Roy. Meteor. Soc.*, **111,** 155–172.

Weickmann, K. M., G. R. Lussky and J. E. Kutzbach, 1985: Intraseasonal (30–60 day) fluctuations of outgoing longwave radiation and 250 mb streamfunction during northern winter. *Mon. Wea. Rev.*, **113,** 941–961.